

Practical guidelines for routine intensity-modulated radiotherapy verification: pre-treatment verification with portal dosimetry and treatment verification with *in vivo* dosimetry

¹A J VINALL, MSc, MIPeM, ¹A J WILLIAMS, PhD, MIPeM, ¹V E CURRIE, MSc, MIPeM, ²A VAN ESCH, PhD and ²D HUYSKENS, PhD

¹Radiotherapy Physics Department, Norfolk and Norwich University Hospitals NHS Foundation Trust, Norwich UK, and ²7 Sigma n.v., Kasteeldreef 2, B-3150 Tildonk, Belgium

ABSTRACT. The purpose of this work is to provide guidelines for the routine use of portal dosimetry and *in vivo* diode measurements to verify intensity-modulated radiotherapy (IMRT) treatments. To achieve tolerance levels that are sensitive enough to intercept problems, both the portal dosimetry and the *in vivo* procedure must be optimised. Portal dosimetry was improved by the introduction of an optimised two-dimensional (2D) profile correction, which also accounted for the effect of backscatter from the R-arm. The scaled score, indicating the fraction of points not meeting the desired gamma evaluation criteria within the field opening, was determined as the parameter of interest. Using gamma criteria of a 3% dose difference and 3 mm distance to agreement, a “scaled score” threshold value of 1.5% was chosen to indicate excessive tongue and groove and other problems. The pre-treatment portal dosimetry quality assurance (QA) does not encompass verification of the patient dose calculation or position, and so it is complemented by *in vivo* diode measurements. Diode positioning is crucial in IMRT, and so we describe a method for diode positioning at any suitable point. We achieved 95% of IMRT field measurements within $\pm 5\%$ and 99% within $\pm 8\%$, with improved accuracy being achieved over time owing to better positioning. Although the careful preparation and setup of the diode measurements can be time-consuming, this is compensated for by the time efficiency of the optimised procedure. Both methods are now easily absorbed into the routine work of the department.

Received 2 March 2009
Revised 22 July 2009
Accepted 29 October 2009

DOI: 10.1259/bjr/31573847

© 2010 The British Institute of
Radiology

In many radiotherapy departments, routine treatment verification for conventional static treatment fields is performed during the first treatment session. This verification often consists of *in vivo* measurements with diodes (mostly on the beam axis) in combination with portal imaging of the treatment-field shapes superimposed on the patient's anatomy. Before the first treatment session, the treatment parameters are carefully reviewed by a qualified person and independent monitor unit (MU) calculations may be performed as an additional check.

For dynamic intensity-modulated radiotherapy (IMRT) fields, a more extensive quality assurance (QA) protocol is considered to be good practice, the reasons for this being at least fourfold:

(1) Both delivery and dose calculations are considerably more complex for dynamic IMRT fields than for conventional static fields.

(2) Conventional portal imaging of the treatment fields provides images that are difficult to interpret because the modulated fluence is superimposed on the patient's anatomy.

(3) Because of the presence of many dose gradients within the IMRT fields, conventional *in vivo* dosimetry on the beam axis is prone to large deviations, or can be meaningless when little dose is delivered on the beam axis.

(4) Dosimetric treatment parameters, such as MU and multileaf collimator (MLC) shape (or movement pattern), depend on the individual patient plan and can vary substantially among patients as a function of the modulation. Hence, statistical prediction of the expected treatment parameters, based on the planner's or radiographer's experience, becomes considerably less straightforward for dynamic IMRT fields than for conventional static fields.

A lot of research and a vast number of publications exist on the subject of IMRT QA [1–17]. IMRT is now also becoming standard practice in smaller, non-academic centres. These centres often have to rely on the commercially available QA solutions because of their limited resources in terms of physicists' time and R&D projects. Table 1 gives an overview of the effectiveness of some of the most commonly used commercial methods for IMRT treatment verification. We have listed possible sources of treatment inaccuracy and given an indicative assessment of the effectiveness of each method in assessing these factors.

The original IMRT QA process relied mostly on ion chamber point dose measurements in combination with

Address correspondence to: Alison Vinall, Radiotherapy Physics Department, Norfolk and Norwich University Hospitals NHS Foundation Trust, Colney Lane, Norwich NR4 7UY, UK. E-mail: Alison.vinall@nnuh.nhs.uk

Table 1. Overview of potential and limitations of various quality assurance methods for assessing routine dynamic intensity-modulated radiotherapy

	Suboptimal MLC parameters	Tongue and groove effect	MLC calibration	MLC single leaf delivery error	Inaccuracies in patient dose calculation algorithm	Overly modulated fluence	Patient setup
Ion chamber point dose	+/-	-	+/-	+/-	+	+/-	-
2D field by field							-
Film	++	++	+	++	+	++	
2D array	+	+/-	+/-	+/-	+/-	+	
2D composite plan	+/-	+/-	+/-	+/-	+/-	+/-	-
Phantom 3D array	+	+/-	+/-	+	+	+	-
Portal dosimetry	++	++	+	++	-	++	-
<i>In vivo</i> dosimetry	+/-	-	-	-	+	+/-	++
MU check programme	+/-	-	-	-	+	+/-	-

MLC, multileaf collimator; 2D, two-dimensional; MU, monitor unit.

++ means that the method is very sensitive to the error; + means that the error should mostly be visible with this method; +/- means that the error could be detected in theory but that it is unlikely to be visible in practice; - means that the error not be detected by this method.

film [1–4]. The ion chamber point dose measurement in itself provides only limited information because it only samples a single point of the 2D dose distribution. If performed with care, however, it provides an absolute dose check point that can be valuable, for example to assure a correct absolute level of an associated film. Because film dosimetry is a cumbersome, time-consuming and error-prone method, it is not a practical solution for most radiotherapy centres. If performed with care and adequate equipment, however, film dosimetry remains one of the more powerful verification methods because of its high resolution and its flexibility in numerous possible phantom setups.

The two-dimensional (2D) ion chamber or diode arrays have become increasingly popular because of their ease of use and reliability [5–9]. In most cases, careful evaluation of the measured and calculated data will detect problems, although deviations of limited spatial extension (such as tongue and groove effects) can be overlooked. Although more efficient than film, these arrays still present a considerable workload in terms of phantom and 2D array setup on the linear particle accelerator. All of the QA methods described above have the advantage that the dose in the phantom can be calculated with the same algorithm used for the patient dose calculation, albeit in a considerably simplified setup. Although a measurement of a composite plan reduces the workload, its sensitivity in detecting problems is less than that offered by field-by-field verification. If problems or discrepancies are found, it is necessary to do a field-by-field verification to try to identify the problem.

Gel dosimetry is the most commonly reported technique for full three-dimensional (3D) IMRT QA [18, 19]. Again, this process is quite cumbersome and MRI time for readout is usually difficult to obtain during normal working hours. New pseudo-3D systems are becoming available. These methods, which are usually referred to as ‘‘3D’’, are actually based on a series of planar measurements from which a 3D dose distribution is recalculated. Although 3D QA methods appear to be of moderate interest for IMRT verification, they are becoming ever more useful for the QA of the upcoming intensity-modulated arc treatments.

The sensitivity of portal dosimetry to error detection largely depends on the specifics of its implementation. The simplest use of portal dosimetry merely provides a visual assessment of the field shape and intensity distribution. The most advanced use is for transit dosimetry, which takes into account not only the behaviour of the machine but also the patient’s anatomy and positioning [12]. As we are focusing on the commercial solutions available at present, the portal dosimetry referred to in Table 1 is the Eclipse TPS (Varian Medical Systems, Palo Alto, CA) pre-treatment solution, albeit calibrated using the improved procedure presented in this work. This offers high-resolution 2D absolute fluence verification: it predicts the expected portal dose image based on the calculated actual fluence distribution for every field. As the actual fluence is also the basic input for the patient dose calculation, this QA method checks an important part of the dose calculation, although not the entire patient dose calculation chain.

Independent MU calculations and *in vivo* point dose measurements do not provide detailed information, but they can be useful in detecting aberrant MLC parameters or clinically relevant errors in the dose calculation algorithm. Like ion chamber point dose measurements, *in vivo* measurement is highly position dependent, even more so because they are acquired on a patient instead of in a simple phantom geometry. However, *in vivo* measurements are the only QA method (listed in Table 1) that is performed during the actual treatment and is therefore sensitive to the actual patient setup.

The available QA methods depend on the implemented IMRT package, which in our case is the full Varian (Varian Medical Systems, Palo Alto, CA) solution. The aim of this work is to provide practical guidelines on optimised data acquisition and analysis for a dynamic IMRT QA protocol based on amorphous silicon (aSi) portal dosimetry in combination with *in vivo* dosimetry with diodes for routine treatments. When opting for this QA tandem, the IMRT verification procedure is very close to the conventional treatment verification procedure, except that the portal image acquisition for visual purposes during the first treatment session of conventional treatments is replaced by a pre-treatment dosimetric portal image acquisition. Table 1 illustrates the

complementary sensitivities of the portal dosimetry and *in vivo* QA procedures.

The portal dosimetry provides an absolute check of the 2D treatment field output dose. Although it is implemented in several different departments as the routine method for IMRT pre-treatment verification [20–27], little information is available in the literature on the criteria to use for the analysis and acceptance/rejection of the acquired data. In addition, the commercially available solution suffers from a suboptimal calibration procedure that limits the achievable accuracy for larger field sizes or highly asymmetrical fields. The first aim of this paper is therefore to present an improved calibration procedure. Analysis of the results of 536 portal dose images from 80 IMRT patients (mostly head and neck patients) was then used to derive a score for the agreement between the calculated and measured portal dose images and to derive tolerance levels (action levels) that allow us to intercept possible problems.

In vivo dosimetry on IMRT patients is often abandoned because the accuracy of *in vivo* dosimetry for IMRT fields can be considerably compromised by the many dose gradients within the treatment field. We believe that *in vivo* measurements can provide a useful complementary check of the portal dosimetry because they verify the absolute point doses obtained directly from the 3D dose calculation on the patient. We have therefore developed a practical method to optimise calculation and measurement precision, together with tolerance levels that can be achieved with this method.

Methods and materials

In our department, we use the integrated Varian solution for IMRT for planning (inverse planning and sliding window leaf motion calculation) and delivery (two Clinac 2100EXs, one Clinac 600EX and one clinic 600CD, all equipped with a 120Millenium MLC). All Clinacs have an aS500 aSi panel with the standard imaging modes and integrated dose acquisition modes. The support arms are all of the R-arm type. IMRT treatment planning is carried out using the Helios module of the Eclipse TPS (v7.5.18). The portal dose images are acquired by the radiographers and the analysis is performed off-line by the physics department. Diode measurements for field entrance doses are carried out routinely for all patients using Scanditronix EPD15 diodes and Invidos software. As an additional independent check of the treatment delivery, 2D array measurements have been performed routinely for all fields by means of the PTW 256 matrix array. The 2D array data are used to cross-check the robustness of both the portal dosimetry and the *in vivo* procedure.

Configuration and calibration of portal dosimetry

For the application of strict gamma evaluation criteria [28], both the mechanical and dosimetric calibration of the imaging machine need to be optimised.

Mechanical calibration

The mechanical calibration procedure for the R-arm on the Clinac was modified in order to obtain good

agreement (tolerance=1 mm) between the central axis (CAX) and the centre of the imager at source-to-imager distance (SID)=105 cm (our default portal dosimetry measurement position). Usually, the imager is calibrated so that the centre of the imager plane coincides with the beam axis at isocentre. However, this does not necessarily mean that they coincide equally well at the clinically used imager distance for portal dosimetry (there is typically a shift of 2–4 mm in the longitudinal direction).

Dosimetric calibration

Most of the flaws in the current portal dosimetry approach within the Varian solution relate to the flood field and profile correction procedure (the aSi pixel sensitivity correction). The official portal dose calibration procedure uses a flood-field correction that is based on the irradiation of the imager panel with an open field (typical field size $40 \times 30 \text{ cm}^2$ at a source–detector distance=105 cm). It then uses a $40 \times 40 \text{ cm}^2$ diagonal field profile measured in water at d_{max} for the profile correction of the beam. This imager calibration method has some significant drawbacks. It results in increasingly large deviations between prediction and measurement towards the edge of the imager because the 40×40 diagonal profile does not describe the penumbra towards the edge of the $40 \times 30 \text{ cm}^2$ field. Second, the mechanical construction of the support arm causes noticeable backscatter for the larger field sizes, especially for the lower energies (6–10 MV) [29]. The backscatter of the arm is inherently included in the flood field correction and is therefore not visible when acquiring an image of a sufficiently large field. However, when the field size is reduced (typically $Y1 < \sim 8 \text{ cm}$) and no direct radiation hits the mechanical bar responsible for the backscatter, the flood field correction still applies a small backscatter correction towards the edge of the field. Third, the spectral dependence of the aSi panel can result in significant errors of up to 10% if the imager is moved off-axis. These deviations were reported by Greer [30] and further investigated by Ko et al [31]. Both showed a large off-axis differential response in the electronic portal imaging device because of spectral sensitivity changes.

No changes were made to the standard dark and flood field calibration. All modifications were included during the dosimetric calibration process (the profile correction and absolute calibration). First, we have applied a 2D profile correction matrix corresponding to the actual field size used during the flood field calibration of the imager. The 2D profile correction is based on a $40 \times 30 \text{ cm}^2$ open field portal dose prediction, which is resampled to map the imager pixels and reformatted to allow its use in the portal dose calibration software. Second, we have chosen to modify the 2D profile correction on the imager in order to visualise the backscatter when it is present, rather than to correct for it even if it is not present (as the latter is less intuitive). The 2D profile correction is therefore multiplied with the effect of the backscatter. The magnitude and location of the backscatter was estimated on the basis of the known mechanical position of the metal parts in the R-arm and on published data [29]. For the R-arm models present in our department, we used a maximum additional backscatter value of 3% for 6 MV and 2% for 10 MV. For both energies, this correction was then validated by means of a series of open field dosimetric

images with fixed $x=38$ cm and increasing $y=2-28$ cm (in steps of 1 cm). As for the spectral dependence, we did not move the imager out of its central position for portal dosimetry, but did use a 90 degree collimator rotation for fields for which Y1 or Y2 exceeded 13 cm. All measured fields fit onto the imager surface at the source of surface distance (SSD)=105 cm.

Statistical analysis of the portal dosimetry

We performed a statistical analysis of the portal dosimetry results acquired with the above-mentioned 2D profile correction for the first 80 IMRT patient scans. Where there are split carriage fields within an IMRT plan, images have to be obtained for each of the individual subfields. The indicated score (iS), as given by Eclipse in the gamma evaluation results, takes all imager pixels into account; therefore, it is always overly optimistic and not a good sensor of possible problems. The parameter investigated in this study is the "scaled score" (sS) of the portal image; this is the percentage of pixels that have a gamma value larger than 1 within the relevant area of the detector. It is calculated from the indicated score:

$$sS = (1 - iS) \times \frac{40 \times 30}{FS \times 1.05^2}$$

where FS is the area of the treatment field.

The gamma value criteria routinely used are 3% dose difference and 3 mm distance to agreement (DTA) [32]. The 3% dose difference criterion is relative to the maximum dose value of the calculated image.

In order to investigate the sensitivity of the scaled score for problem detection, additional data were acquired for IMRT fields into which deliberate errors or problems had been introduced, such as very asynchronous MLC movements resulting in large tongue and groove effects, suboptimal MLC parameters and a blocked MLC movement to simulate a leaf motion error.

IMRT-optimised in vivo dosimetry

Diode measurements for field entrance doses are carried out routinely in this department for all 3D conformal patients using Scanditronix EPD 15 diodes and Invidos software. For static fields, the diode is placed on the central

axis of the beam. This is not usually appropriate for IMRT treatments; therefore, we have developed a procedure to position the diode on a high-dose-low-dose gradient point anywhere within the field and in an accessible and reproducible position on the patient.

Where there are split carriage fields within an IMRT plan, a diode measurement is obtained for the total field. For some posterior oblique head and neck treatment fields, no measurements could be made because of difficulties with the positioning of the diode.

A "diode" plan is created for each patient from a copy of the original IMRT plan and scheduled alongside the treatment plan. A suitable point of measurement is then chosen for each field in beam's-eye view (BEV) mode. A high-dose-low-gradient area can be selected from the 2D fluence display in the BEV. The underlying 3D surface contours of the patient's body outline allow simultaneous assessment of the anatomical suitability of the chosen point, ensuring, for example, that the corner of the mouth and the sloping gradient of the posterior neck are avoided. In addition, it is used to measure the SSD to the point of diode placement and the angle of incidence (AOI) of the diode with the beam. The diode dose is measured at d_{max} in the patient and normal correction factors for *in vivo* diodes are applied, for example SSD, AOI, energy and temperature.

The dynamic MLC is then replaced by a static MLC with very small field openings (0.5 cm^2) to project the diode measurement position onto the patient (Figure 1). The fields of the diode plan are converted into setup fields to make sure that no accidental dose can be given with these fields. Once the diode has been properly placed onto the patient by means of this small light field projection, the treatment field can be activated and delivered.

Results

Portal dosimetry

Figure 2 compares the predicted and measured open field portal dose profiles of a $40 \times 30 \text{ cm}^2$ (Figure 2a) and a $10 \times 10 \text{ cm}^2$ field (Figure 2b). Measurements were acquired with the official diagonal profile correction and a modified 2D profile correction, with and without

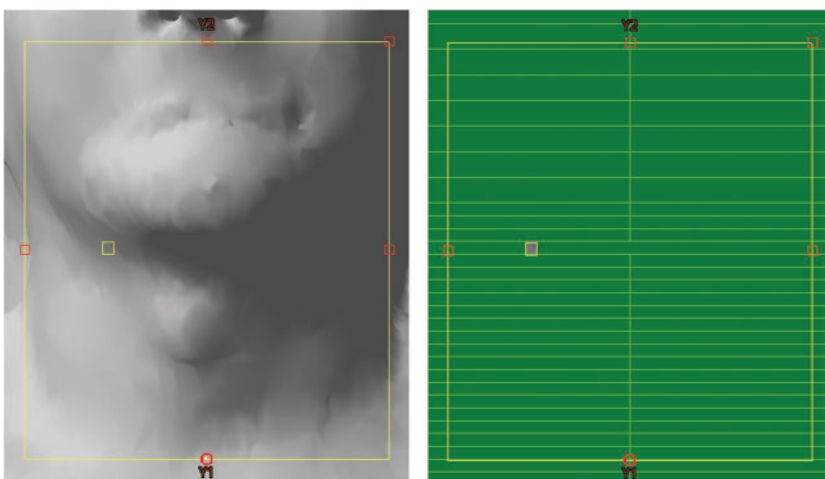


Figure 1. Use of patient anatomy and the MLC to project the diode position onto the patient at a suitable location.

backscatter correction. The effects are most pronounced — and therefore displayed — along the longitudinal direction. First, the official profile correction procedure shows deviations of up to 8% towards the edge of the imager panel, but agreement with the 2D profile correction without backscatter is by definition near-perfect for the $40 \times 30 \text{ cm}^2$ field. For the $10 \times 10 \text{ cm}^2$ field profile, almost no difference is observed between the official and 2D correction, both showing the almost wedge-like asymmetry caused by an inappropriate backscatter compensation (Figure 2b). Introducing the backscatter into the 2D profile correction removes this unwanted effect for the $10 \times 10 \text{ cm}^2$ field, while displaying the additional back-scattered dose when the field size is large enough to take in the R-arm. For the large field sizes, the observed deviation between calculated and measured data is now as expected: maxima of 3% and 2% for 6 MV and 10 MV, respectively. Figure 2c also shows a $10 \times 10 \text{ cm}^2$ field measured with the imager in its central position and with a longitudinal position of 10 cm off-axis; here, the effect of moving off-axis is dramatic.

The histogram distribution of the scaled scores for the 80 patients (536 fields) is given in Figure 3, which also includes the scaled score for each of the problem-induced test cases. The majority of the fields obtain a scaled score that does not exceed 1.5%. For these fields, careful visual analysis confirmed excellent overall agreement with no significant areas of deviations. The 2D array measurements showed equally good agreement. The presence of tongue and groove causes a noticeable increase in the *sS* value (2–3.5%). The tongue and groove can easily be recognised from its characteristic narrow stripes in the 2D gamma display (Figure 4a). Although the 2D array data for these fields also show a somewhat inferior agreement between calculated and measured dose planes, the tongue and groove diagnosis cannot be made with equal ease because of the inferior resolution of the array. The fields with artificially induced errors also show an unmistakable increase in the *sS* values. Figure 4b displays the impact of not assigning the appropriate MLC parameters to the Eclipse dose calculation algorithm, leading to an alarmingly high score of 36.3%. If only one of the transmission or dosimetric leaf separation values is set to zero then the scaled score is approximately 10%. It is this value that is indicated in Figure 3. The simulated single leaf error yields a score of 6.8% and the 2D gamma image readily displays the faulty leaf. Both problems were also intercepted by the 2D array measurements.

In addition, significantly higher scaled scores were found for a few clinical fields. Closer inspection of the portal dose images of these fields showed that the affected fields are all low-dose subfields of a multiple carriage delivery. The main part of the total field dose was delivered by the complementary carriage group and only a very small fraction (dosimetrically as well as geometrically) was actually delivered through the field with the high *sS*. Therefore, a large part of the dose within the field opening is purely delivered through leaf transmission. Visual evaluation of the portal dose images showed good agreement in the area irradiated through the opened moving leaves, but poor agreement in the area of transmission dose. Summed 2D array measurements were acquired by leaving the measurement

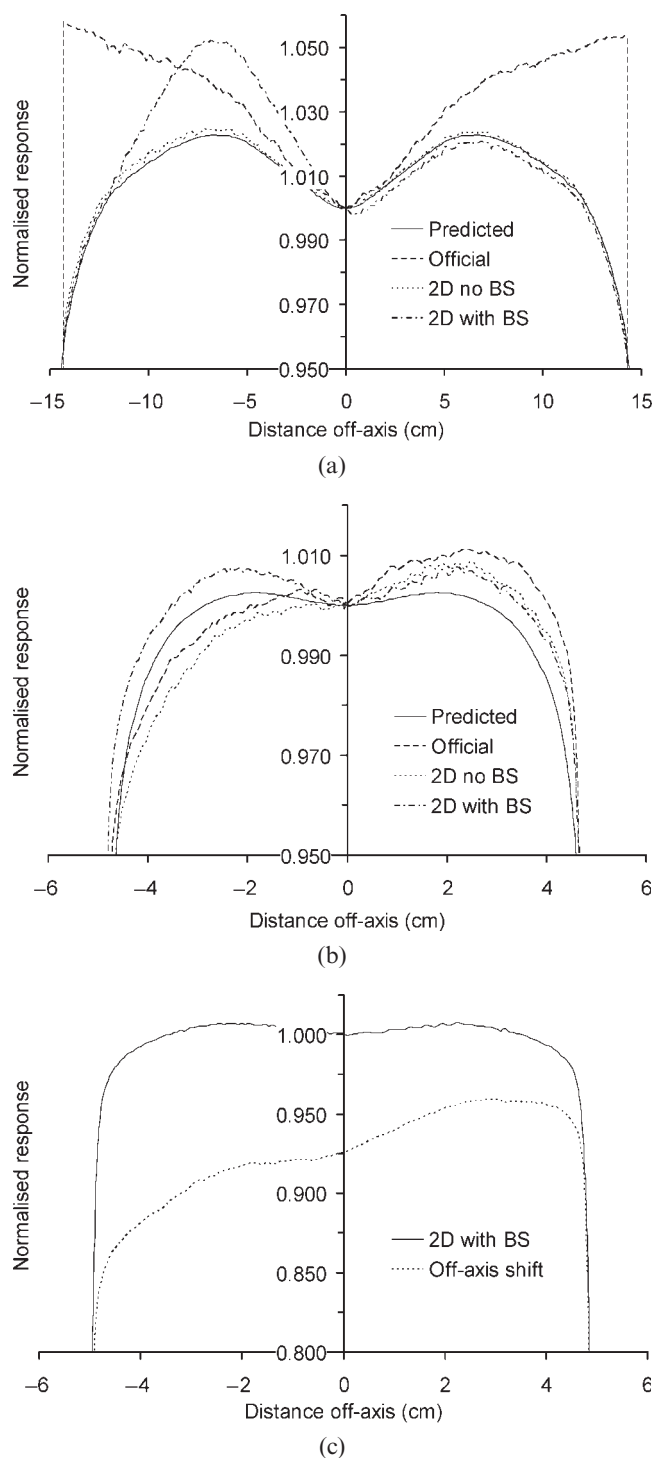


Figure 2. Predicted and measured open field portal dose profiles. (a) 40×30 field, (b) 10×10 field and (c) 10×10 field off axis; BS, baseline shift; 2D, two dimensional.

running when proceeding from the first to the second carriage group. The 2D array data did not show these discrepancies and all of the above-mentioned fields were well within the gamma acceptance criteria.

In vivo dosimetry

From the 80 patients, diodes were used to measure the entrance dose for 437 fields out of a possible 480 fields. 377 fields were IMRT fields and 60 fields were matched

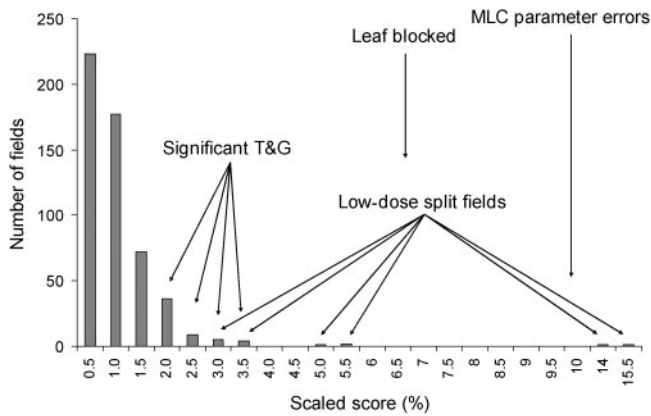


Figure 3. Number of intensity-modulated radiotherapy fields vs “scaled score” i.e. % gamma value > 1 . T&G, tongue and groove; MLC, multileaf collimator.

static anterior split neck fields. Figure 5a illustrates the results for IMRT fields. For nearly all acquired data, the difference between the planned and measured point doses was within $\pm 5\%$ (mean = -0.8% , SD = 2.8%). Static asymmetrical matched neck fields for the same patients also had entrance dose measurements ($n=60$, mean = -1.5% , SD = 1.8%). All 60 neck measurements are within $\pm 5\%$ of the predicted entrance dose.

When evaluating the total number of measured fields as well as the number of fields with a deviation larger than 5% as a function of time, we noticed that the number of deviating fields decreased considerably over a period of 42 months after the initial start-up of the QA protocol (Figure 5b).

Discussion

Figure 2 clearly illustrates the consequences of the simplified calibration procedure in the Varian portal dosimetry QA package. As can be seen from the $40 \times 30 \text{ cm}^2$ field data, good agreement (3%, 3 mm) between measured and calculated images can be expected only for fields of moderate size ($< \sim 15 \times 15 \text{ cm}^2$). For fields that extend beyond the central area of the imager panel, the deviations seen in the open field will superimpose on all other possible deviations for IMRT fields. For highly asymmetrical fields, such as the head and neck half-fields used in our department, it might be tempting to move the imager panel such that the field covers the central area of the detector again. Unfortunately, this is not a solution as the spectral dependence of the aSi will only make matters worse. The increased sensitivity towards lower energies is calibrated out during the flood-field correction, which is performed with the imager panel in its central position and is therefore valid only in this central position. Although noticeable in the static open fields, the effect of the backscatter of the R-arm is less obvious when superimposed on the modulated clinical fields.

After introducing the 2D profile correction matrix, the results for large and/or highly asymmetrical treatment fields improve considerably. The main improvement comes from the use of a 2D profile correction that is based on the correct field size rather than from the one-dimensional (1D) diagonal profile correction for $40 \times 40 \text{ cm}^2$

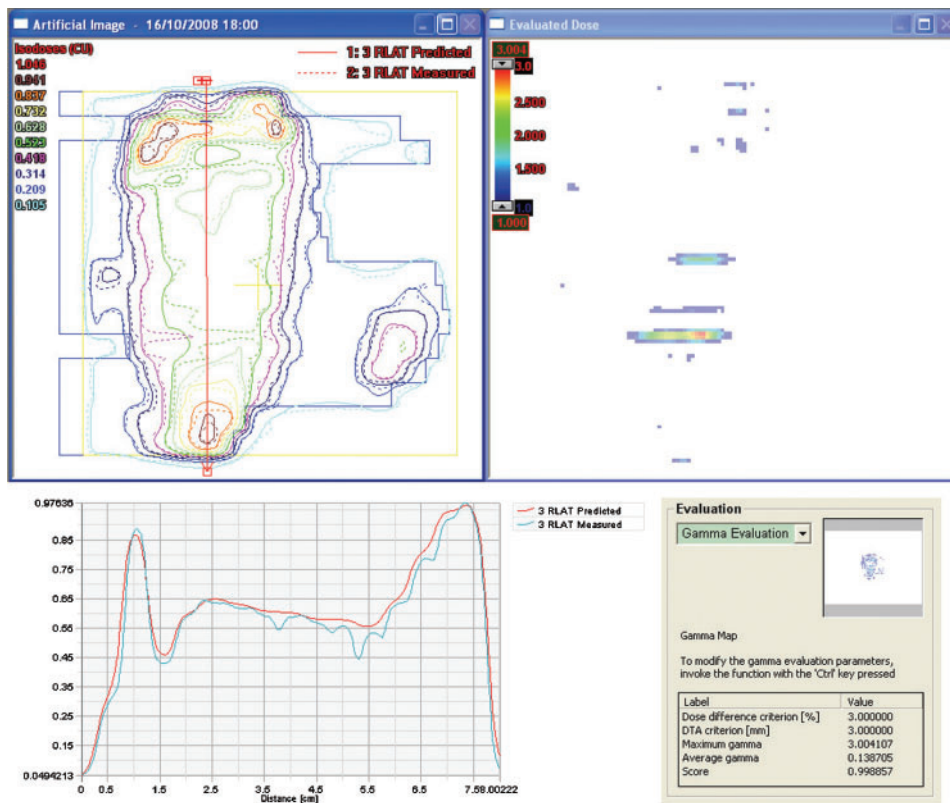
at d_{max} in water. For this 2D profile correction, we have taken a rather pragmatic approach by introducing the $40 \times 30 \text{ cm}^2$ portal dose prediction into the actual measurement calibration. As such, we map the measurement to the prediction for the largest possible field size. As alternative approaches, the 2D profile map can be reconstructed from in-line and cross-line profiles for a $38 \times 29 \text{ cm}^2$ field acquired at 8 mm depth in water by film or by Monte Carlo calculations. The first of these approaches was used by Van Esch et al [26] during the original development of the portal dose prediction algorithm. We have opted to use the predicted open field portal dose as the basis for the 2D correction because our primary interest in the portal dosimetry is IMRT verification, not open field validation. It is therefore desirable to make the open fields agree as much as possible. Unfortunately, on the imager side, there is no profile correction that can account for the backscatter for all field sizes. The only way to take the backscatter into account correctly would be to introduce its effect into the prediction. As this is not possible in the current version of the prediction algorithm, such a correction would require exporting the images and manipulating them in external software. We have therefore chosen to modify the 2D profile correction on the imager in order to visualise the backscatter when it is present. This approach mostly improves the agreement between predictions and calculations for moderately modulated fields in the order of $7 \times 7 \text{ cm}^2$ to $15 \times 15 \text{ cm}^2$. The introduced backscatter is hardly noticeable in the larger head and neck fields because the 2–4% additional dose bump fades away into the many high gradient areas of these highly modulated fields.

The only real solution to the spectral dependence of the imager would be an entirely revised flood-field calibration procedure and an off-axis modelling of the spectral effects in the portal dose prediction, as described by Greer [30]. When open field agreement up to the very edge of the detector panel is improved, however, the spectral dependence becomes less of an issue because the clinical fields can use the whole surface of the detector and the need to move the imager panel off-axis is reduced.

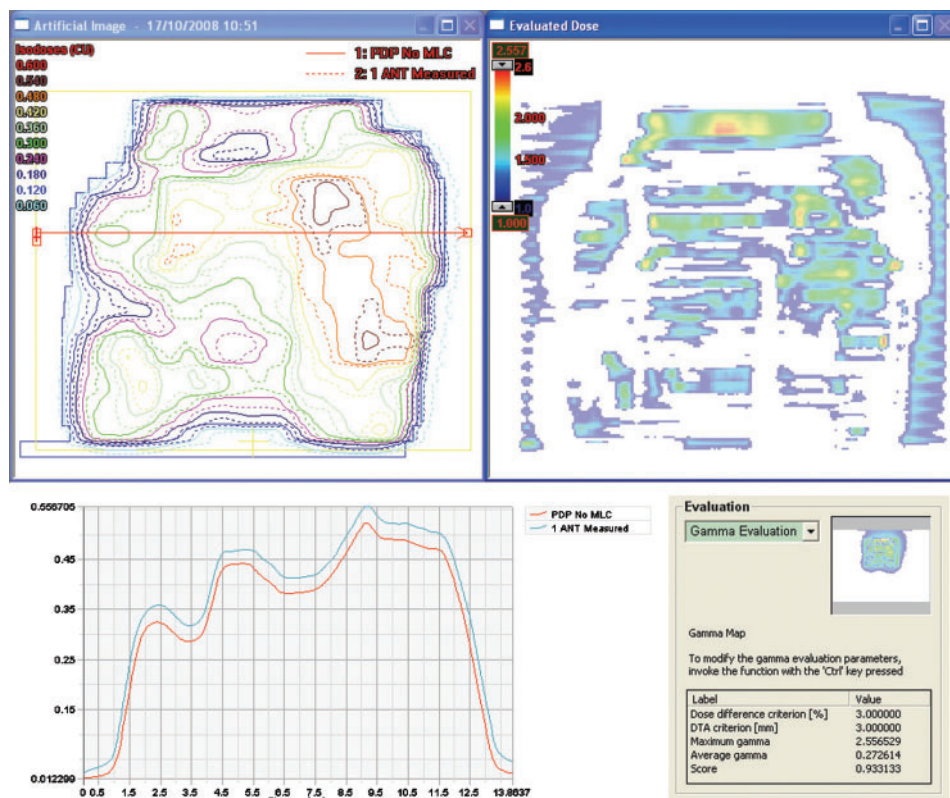
Having optimised the portal dosimetry QA method as much as possible within the existing software, that is without compromising the method's efficacy, we then aimed to derive pass/fail criteria and action levels for the rejection/validation of the portal dosimetry data for routine IMRT QA.

From the analysis of the gathered patient data set, based on the 3%, 3 mm criteria commonly used for IMRT, we propose a tolerance level of 1.5% for the scaled score. Portal dose images with a scaled score exceeding this value should be subjected to further investigation. This action level for the score is selected to ensure that possible errors or problems are detected, even if this implies the occasional false alarm. The score seems to be a good parameter to intercept errors: sub-optimal MLC parameters or a mechanical problem with the MLC lead to significantly higher scaled scores. If a significant tongue and groove appears to be the cause of the high score, one single score is probably not sufficient to assess clinical acceptability as the cumulative effect of all fields would need to be taken into account.

Suboptimal agreement caused by backscatter of the R-arm is characterised by its unchanging location on the



(a)



(b)

Figure 4. (a) Sensitivity to tongue and groove effect. The scaled score for the above illustration of sensitivity to the tongue and groove effect is 2.1%. (b) Sensitivity to erroneous multileaf collimator (MLC) parameters. The scaled score for this illustration of sensitivity to the suboptimal MLC parameters is 36.3%.

imager panel. In case of doubt, the portal dosimetry can be repeated with a collimator rotation of 90 degrees. If caused by backscatter, the area of suboptimal agreement will not rotate correspondingly. If the field with the high score appears to be a low-dose subfield of a multiple carriage field, visual verification by means of line profiles often reveals that the out of tolerance area coincides with the part of the field that remains covered by the MLC leaves during beam-on. It should be noted that the proposed criteria can be met only when using the improved calibration method. With the official calibration procedure, comparable values for the scaled score are only obtained for fields irradiating the central part of the detector.

Our *in vivo* dosimetry programme for treatment verification provides a complementary means to verify the patient dose calculation, patient setup and the treatment unit performance. To date, there is little reported information on the use of diodes for IMRT treatment verification. Higgins et al [33] report 90% of diode measurements agreeing to within $\pm 10\%$ of planned doses and 63% achieving $\pm 5\%$. The agreement reported here is better: 95% of all IMRT fields are within a standard treatment tolerance of $\pm 5\%$ and 99% within $\pm 8\%$. Higgins et al [33] discussed the potential complication of scatter conditions in the use of dynamic MLC IMRT

techniques but found no significant differences in diode response between dynamic MLC techniques and step and shoot techniques. Although their results are for step and shoot IMRT, we have shown similar results for dynamic IMRT. For all entrance dose measurements, the expected accuracy of the diodes has been estimated as $\pm 2.9\%$ based on all the uncertainties added in quadrature. The tolerance levels are $\pm 4\%$ for conventional head and neck treatments, and $\pm 5\%$ for all other body sites. This corresponds to values used in other departments [34].

The action level for investigation of IMRT diode results has been set slightly higher at $\pm 5\%$ because of the increased sensitivity of diode positioning but remains at a level useful to detect significant errors. Diode placement in an area of high-dose gradient and low dose is the most common cause of measurements outside the $\pm 5\%$ tolerance level. However, the increased use of *in vivo* dosimetry over the period of 42 months during which the 80 patients were treated led to a decrease in the number of measurements outside the $\pm 5\%$ tolerance level.

Conclusion

A comprehensive QA programme for IMRT patients has been introduced in our department that is based on the combination of pre-treatment portal dosimetry for fluence verification and *in vivo* diode measurements for patient dose and patient setup verification. The standard portal dosimetry solution is modified with an optimised 2D profile correction, taking into account the actual field size during calibration and the backscatter effect of the imager arm. For all fields, the scaled score is calculated, indicating the number of points that have failed the 3%, 3 mm gamma evaluation within the field opening. From a statistical analysis of the scaled score, a value of 1.5% was derived as the threshold value above which further investigation is desirable if possible problems are to be intercepted. For IMRT treatment verification, a dedicated *in vivo* dosimetry programme with diodes has been implemented. As *in vivo* dosimetry on the beam axis is not possible, we use a dedicated plan in which the light field of the MLC is used to position the diode. Our results show that with this setup, a tolerance/action level of $\pm 5\%$ can be used.

We have reduced our IMRT QA time for portal dosimetry to 20 min data acquisition per patient (calculation, measurement and scaled score calculation), all carried out by radiographers. Should the scaled score exceed the tolerance level of 1.5%, the case is transferred to the physicist for further investigation. This is a significant reduction on other reported IMRT QA time schedules [13, 14, 25]. Although the preparation of the small MLC fields may take up to 1 h in treatment planning, their use facilitates precise diode positioning during the first treatment session. As our results show a significant increase in accuracy over levels reported previously [33], we consider this to be a worthwhile investment in patient safety.

References

- Boehmer D, Bohsung J, Eichwurzels I, Moys A, Budach V. Clinical and physical quality assurance for intensity modulated radiotherapy of prostate cancer. *Radiation Oncol* 2004;7:1:319-25.

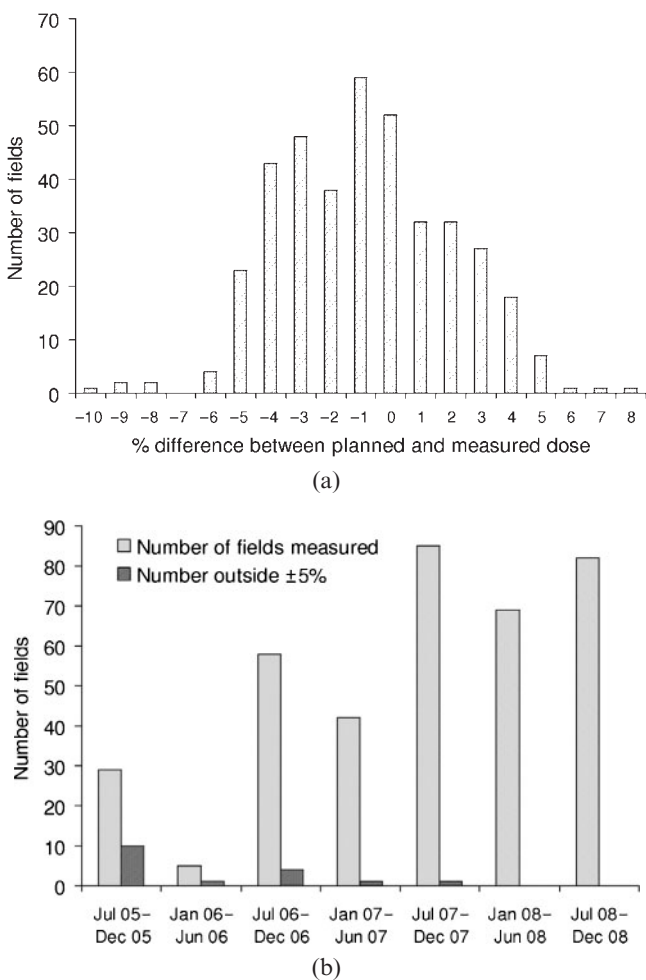


Figure 5. Entrance dose measurements for 80 intensity-modulated radiotherapy (IMRT) patients. (a) IMRT fields only and (b) improved diode accuracy with time owing to increased positioning accuracy.

2. Clark CH, Mubata CD, Meehan CA, Bidmead AM, Staffurth J, Humphreys ME, et al. IMRT clinical implementation: prostate and pelvic node irradiation using Helios and a 120-leaf multileaf collimator. *J App Clin Med Phys* 2002;3:273–84.
3. Ezzell GA, Galvin JM, Low D, Palta JR, Rosen I, Sharpe MB, et al. Guidance document on delivery, treatment planning, and clinical implementation of IMRT: Report of the IMRT subcommittee of the AAPM radiation therapy committee. *Med Phys* 2003;30:2089–115.
4. Bucciolini M, Buonamici FB, Casati M. Verification of IMRT fields by film dosimetry. *Med Phys* 2004;31:161–8.
5. Jursinic P, Nelms B. A 2-D diode array and analysis software for verification of intensity modulated radiation therapy delivery. *Med Phys* 2003;30:870–9.
6. Letourneau D, Gulam M, Yan D, Oldham M, Wong JW. Evaluation of a 2D diode array for IMRT quality assurance. *Radiother Oncol* 2004;70:199–206.
7. Spezi E, Angelini AL, Romani F, Ferri A. Characterization of a 2-D ion chamber array for the verification of radiotherapy treatments. *Phys Med Biol* 2005;50:3361–73.
8. Wieszorek T, Banz N, Schwedas M, Scheithauer M, Salz H, Georg D, et al. Dosimetric quality assurance for intensity-modulated radiotherapy. *Strahlenther Onkol* 2005;181:468–74.
9. Poppe B, Blechschmidt A, Djouguela A, Kollhoff R, Rubach A, Willborn K, et al. Two dimensional ionization chamber arrays for IMRT plan verification. *Med Phys* 2006;33:1005–15.
10. McDermott LN, Wendling M, van Asselen B, Stroom J, Sonke J-J, van Herk M, et al. Clinical experience with EPID dosimetry for prostate IMRT pre-treatment dose verification. *Med Phys* 2006;33:3921–30.
11. van Elmpt W, McDermott L, Nijsten S, Wendling M, Lambin P, Mijnheer B. A literature review of electronic portal imaging for radiotherapy dosimetry. *Radiother Oncol* 2008;88:289–309.
12. Wendling M, Louwe RJW, McDermott LN, Sonke J-J, van Herk M, Mijnheer BJ. Accurate two-dimensional IMRT verification using a back-projection dosimetry method. *Med Phys* 2006;33:259–73.
13. Kapulsky A, Mullokandov E, Gejerman G. An automated phantom-film QA procedure for intensity-modulated radiation therapy. *Med Dosim* 2002;27:201–7.
14. Van Esch A, Bohsung J, Sorvari P, Tenhunen M, Paiusco M, Iori M, et al. Acceptance tests and quality control (QC) procedures for the clinical implementation of intensity modulated radiotherapy (IMRT) using inverse planning and the sliding window technique: experience from five radiotherapy departments. *Radiother Oncol* 2002;65:53–70.
15. Childress NL, White RA, Bloch C, Salehpour M, Dong L, Rosen II. Retrospective analysis of 2D patient-specific IMRT verifications. *Med Phys* 2005;32:838–50.
16. Depuydt T, Van Esch A, Huyskens DP. A quantitative evaluation of IMRT dose distributions: refinement and clinical assessment of the gamma evaluation. *Radiother Oncol* 2002;62:309–19.
17. Budgell GJ, Perrin BA, Mott JHL, Fairfoul J, Mackay RI. Quantitative analysis of patient-specific dosimetric IMRT verification. *Phys Med Biol* 2005;50:103–19.
18. Crescenti RA, Scheib SG, Schneider U, Gianolini S. Introducing gel dosimetry in a clinical environment: customization of polymer gel composition and magnetic resonance imaging parameters used for 3D dose verifications in radiosurgery and intensity modulated radiotherapy. *Med Phys* 2007;34:1286–97.
19. Wu CS, Xu Y. Three-dimensional dose verification for intensity modulated radiation therapy using optical CT based polymer gel dosimetry. *Med Phys* 2006;33:1412–19.
20. Greer PB, Popescu CC. Dosimetric properties of an amorphous silicon electronic portal imaging device for verification of dynamic intensity modulated radiation therapy. *Med Phys* 2003;30:1618–27.
21. Grein E, Lee R, Luchka K. An investigation of a new amorphous silicon electronic portal imaging device for transit dosimetry. *Med Phys* 2002;29:2262–8.
22. Louwe R, McDermott L, Sonke J-J, Tielenburg R, Wendling M, van Herk MB, et al. The long term stability of amorphous silicon flat panel imaging devices for dosimetry purposes. *Med Phys* 2004;31:2989–95.
23. Nicolini G, Fogliata A, Vanetti E, Clivio A, Cozzi L. GLAaS: an absolute dose calibration algorithm for an amorphous silicon portal imager. Applications to IMRT verifications. *Med Phys* 2006;33:2839–51.
24. Steciw S, Warkentin B, Rathee S, Fallone BG. Three-dimensional IMRT verification with a flat-panel EPID. *Med Phys* 2005;32:600–12.
25. Talamonti C, Casati M, Bucciolini M. Pre-treatment verification of IMRT absolute dose distributions using a commercial a-Si EPID. *Med Phys* 2006;33:4367–78.
26. Van Esch A, Depuydt T, Huyskens DP. The use of an aSi-based EPID for routine absolute dosimetric pre-treatment verification of dynamic IMRT fields. *Radiother Oncol* 2004;71:223–34.
27. Van Zijtveld M, Dirckx MLP, de Boer HCJ, Heijmen BJM. Dosimetric pre-treatment verification of IMRT using an EPID; clinical experience. *Radiother Oncol* 2006;81:168–75.
28. Low DA, Harms WB, Mutic S, Purdy JA. A technique for the quantitative evaluation of dose distributions. *Med Phys* 1998;25:656–61.
29. Siebers JV, Kim JO, Ko L, Keall PJ, Mohan R. Monte Carlo computation of dosimetric amorphous silicon electronic portal images. *Med Phys* 2004;31:2135–45.
30. Greer P. Correction of pixel sensitivity variation and off-axis response for amorphous silicon EPID dosimetry. *Med Phys* 2005;32:3558–68.
31. Ko L, Kim JO, Siebers JV. Investigation of the optimal backscatter for an aSi electronic portal imaging device. *Phys Med Biol* 2004;49:1723–38.
32. Stock M, Kroupa B, Georg D. Interpretation and evaluation of the γ index and the γ index angle for the verification of IMRT hybrid plans. *Phys Med Biol* 2005;50:399–411.
33. Higgins PD, Alaei P, Gerbi BJ, Dusenbery KE. *In vivo* diode dosimetry for routine quality assurance in IMRT. *Med Phys* 2003;30:3118–23.
34. Huyskens D, Bogaerts R, Verstraete J, Loof M, Nystrom H, Fiorino C, et al. Practical guidelines for the implementation of *in-vivo* dosimetry with diodes in external radiotherapy with photon beams (entrance dose). ESTRO Booklet No. 5. Belgium: Garant, 2001.